Icarus 250 (2015) 430–437

Contents lists available at ScienceDirect

Icarus

journal homepage: www.elsevier.com/locate/icarus

Potentially hazardous Asteroid 2007 LE: Compositional link to the black chondrite *Rose City* and Asteroid (6) Hebe

Sherry K. Fieber-Beyer [a,*,1], Michael J. Gaffey [a,1], William F. Bottke [b], Paul S. Hardersen [a,1]

[a] Department of Space Studies, University Stop 9008, University of North Dakota, Grand Forks, ND 58202, USA
[b] Southwest Research Institute, NASA Lunar Science Institute, 1050 Walnut St., Suite 300, Boulder, CO 80302, USA

ARTICLE INFO

Article history:
Received 28 March 2014
Revised 15 December 2014
Accepted 16 December 2014
Available online 24 December 2014

Keywords:
Asteroids
Near-Earth objects
Asteroids, composition
Infrared observations
Mineralogy

ABSTRACT

The research is an integrated effort beginning with telescopic observations and extending through detailed mineralogical characterizations to provide constraints on the albedo, diameter, composition, and meteorite affinity of near-Earth object-potentially hazardous asteroid (NEO-PHA 2007 LE). Results of the analysis indicate a diameter of 0.56 kilometers (km) and an albedo of 0.08. 2007 LE exhibits a 1-μm absorption feature without a discernible Band II feature. Compositional analysis of 2007 LE reveal Fs_{17} and Fa_{19} values, which are consistent with the Fa and Fs values for the H-type ordinary chondrites ($Fs_{14.5–18}$ and $Fa_{16–20}$) and of Asteroid (6) Hebe (Fs_{17} and Fa_{15}). Spectroscopically, 2007 LE does not appear like the average H-chondrite spectra, exhibiting a reddened spectrum and subdued absorption feature. Further investigation of the meteorite classes yielded a black chondrite, *Rose City*, which is both similar in mineralogy and spectrally to PHA 2007 LE. Dynamical analysis could not directly link the fall of the *Rose City* meteorite to 2007 LE. As it stands, 2007 LE and *Rose City* have a compositional link, and both could come from the same parent body/possible family, one known source of the H chondrites is (6) Hebe.
© 2015 Elsevier Inc. All rights reserved.

1. Introduction

Although there is general agreement that most meteorites are samples of asteroids, the identification of the specific asteroid parent bodies of individual meteorites or of meteorite types has been a high priority in asteroid science for nearly five decades. Establishment of such links allows the detailed chemical, isotopic and chronological characterizations of meteorite samples in terrestrial laboratories to be placed into a spatial context in the present Solar System, and via dynamical models into a spatial context in the early Solar System. Although many asteroid–meteorite links have been suggested in the past only a few have survived the test of time. Of the ~135 different asteroidal parent bodies represented in the meteorite collections, only a few types have parent bodies identified, with varying degree of certainty. The most agreed upon connection is between Asteroid 4 Vesta and the HED meteorites (McCord et al., 1970 & results of the DAWN mission). Spectrally, the near-Earth Asteroid (3103) Eger and the enstatite achondrites/aubrites are similar (Gaffey et al., 1992), and this may suggest a connection between these meteorites and Eger-like bodies in the Hungaria asteroid family. Interesting links have also been proposed between the LL chondrites and the Flora family (Vernazza et al., 2008), the L chondrites and the Gefion family (Nesvorný et al., 2009), and the mesosiderites and the Maria Family (Fieber-Beyer et al., 2011). It is probable that the H-chondrites and IIE irons came from (6) Hebe (Gaffey and Gilbert, 1998), though caveats exist (e.g., Rubin and Bottke, 2009). The identification of many more large asteroids with H chondrite-like spectra also means that more candidates are now available to serve as a source for these meteorites (Vernazza et al., 2014).

A meteorite may derive from a meteoroid released from a main belt parent body or parent family which then undergoes orbital evolution to put it into an Earth encountering orbit. The meteoroid may also be released from an object already in an Earth-approaching orbit such as a near-Earth object (NEO). In the latter case, the NEO would be an intermediate precursor between the primary main belt parent body and the meteoroid.

On June 2, 2007 the NEO 2007 LE, was discovered by the LINEAR NEO survey and subsequently designated as a PHA (potentially hazardous asteroid) by The Minor Planet Center. On June 03, 2012 UT, 2007 LE passed within 0.049 AU of the Earth. At the time, nothing but the absolute visual magnitude (H) magnitude was known which provided a rough estimate of diameter (D_{eff}). Most

* Corresponding author.
E-mail address: sherryfieb@hotmail.com (S.K. Fieber-Beyer).
[1] Visiting Astronomer at the Infrared Telescope Facility, which is operated by the University of Hawaii under Cooperative Agreement no. NNX-08AE38A with the National Aeronautics and Space Administration, Science Mission Directorate, Planetary Astronomy Program.

http://dx.doi.org/10.1016/j.icarus.2014.12.021
0019-1035/© 2015 Elsevier Inc. All rights reserved.

NEO sizes are not actually measured, but are estimated based on the absolute visual magnitude (H) and assumed albedos of 0.05 and 0.25, which corresponds to a factor of 2.2 uncertainty in the estimated diameter and an uncertainly of a factor of 11 in the estimated mass of an NEO. Analysis of NEO data from the WISE satellite has provided size determinations for a few percent of the NEO population (e.g., Mueller et al., 2011; Mainzer et al., 2012). Radar observations are also used to obtain measurements of asteroid shapes, spins, masses, densities, and trajectories. Taxonomic classifications, including ambiguous types, are also available for a few percent of the known NEO population (e.g., Binzel et al., 2004; Fevig and Fink, 2007; DeMeo et al., 2009). Actual compositional determinations and/or identified meteorite analogs are available for less than 1% of the known NEO population. Although most NEOs are believed to originate from collision events on asteroids in the mainbelt, the pathways of these fragments into Earth-crossing orbits are known only in a statistical way.

Sophisticated mineralogical characterizations are critical to establishing the physical nature of individual NEOs and of NEO subpopulations such as the PHAs. While taxonomy provides broad insights into the relationships of asteroid groups, taxonomic classification is not a compositional interpretation. Objects in different taxonomic classes are likely to be composed of different materials, but there is no assurance that objects of the same taxonomic type are composed of similar materials. Mineralogical characterizations are the key to unraveling the history and relationships between asteroids, their parent bodies, and the meteorites derived from them. The research reported here is an integrated effort beginning with telescopic observations and extending through detailed mineralogical characterizations to provide constraints on the albedo, diameter, composition, and meteorite affinity of 2007 LE.

2. Observations/data reduction

Near-infrared spectral observations were obtained at the NASA Infrared Telescope Facility located at Mauna Kea Observatory, Hawai'i. The observational parameters from the observing run are listed in Table 1. Physical properties and orbital elements are listed in Table 2. The spectra were obtained using the facility SpeX instrument in the low-resolution spectrographic mode (Rayner et al., 2003).

A local G-type standard star was selected to provide both a spectral flux calibration and to track the varying atmospheric absorption during the asteroid observations. Asteroid and local standard star spectra were acquired in interspersed sets of ten. A solar analog star was also observed to provide a calibration standard. Extraction of spectra, determination of wavelength calibration, and data reduction were done using procedures outlined by (Clark, 1980; Hardersen et al., 2005; Reddy, 2009; Fieber-Beyer, 2010). Individual raw flux spectra were corrected to a standard pixel array to compensate for the (generally) subpixel shifts of the dispersed spectrum on the array detector (e.g., Gaffey et al., 2002). The first spectrum of each set was discarded due to image persistence on the detector chip and other spectra were discarded due to poor quality because of deteriorating weather conditions.

The local standard star data were used to derive the extinction coefficients ("starpacks") from the variation in flux versus air mass (atmospheric path length) for each channel in the spectrum. Starpacks were computed for various permutations of the standard star observations (e.g., all standard star sets, sets that bracketed individual sets of asteroid observations, etc.).

Each asteroid flux curve was divided by the several permutations of starpacks to identify the starpack that most effectively removed the atmospheric water vapor features to produce a final spectrum. The individual spectra for 2007 LE were averaged, deleting individual points that deviated by more than two standard deviations from the mean. The PHA's average spectrum was then ratioed to an average of the solar analog spectra for its respective night to correct for any non-solar spectral properties of the local standard star.

The position of the absorption features (band centers) and the relative areas of the features (band area ratios, BAR) are diagnostic of the compositions and abundances of mafic silicates (e.g., Adams, 1974, 1975; Cloutis et al., 1986; Gaffey et al., 1993, 2002; Gastineau-Lyons et al., 2002; Burbine et al., 2003, 2009; Dunn et al., 2010). The near-infrared spectrum of 2007 LE exhibits a single absorption feature in the 1 μm region (Fig. 1). The band center (0.94 ± 0.02 μm – Table 3) was measured relative to a linear continuum fitted tangent to the spectral curve outside the absorption feature (e.g., Cloutis et al., 1986). The uncertainty was estimated from several polynomial fits, sampling different ranges of points within the Band I spectral interval (i.e. points sampled to the left and right of the center of the feature, deleting any spurious outlying points). The uncertainty was determined as half the difference between the minimum and maximum values calculated from the polynomial fits.

Temperature affects the band center positions of mafic minerals such as pyroxene (e.g., Roush, 1984; Roush and Singer, 1986; Lucey et al., 1998; Moroz et al., 2000; Hinrichs and Lucey, 2002; Sunshine et al., 2007; Reddy et al., 2011). The Dunn et al. (2010) calibration used below was based on laboratory spectra of ordinary chondrites measured at room temperature (~290 K). We calculated the surface temperature of 2007 LE using the formula from Burbine et al. (2009):

$$T = [(1 - A)\mathrm{Lo}/16\eta\varepsilon\sigma\pi r2]1/4$$

where A is the asteroid albedo, Lo is the solar luminosity (3.846×10^{26} W), η is the beaming factor (assumed to be 1.0), ε is the asteroid's infrared emissivity (assumed to be 0.9), σ is the Stefan–Boltzmann constant, and r is the asteroid's distance from the Sun in meters. For our derived albedo of 8% (see below), the surface temperature of 2007 LE at a heliocentric distance of 1.058 AU would be 272 K. An increase or decrease of the albedo to 0.09 or 0.07 would only change the temperature by ~1–2°. The ~20 K lower temperature for the asteroid surface compared to the laboratory calibration samples would produce a shift in the Band position of ~−0.002 μm using the calibration for orthopyroxenes by Roush

Table 2
Orbital and physical properties.

Object	a (AU)[a]	e[a]	i (°)[a]	D_{eff} (km)[b]	Albedo[b]	H[a]
2007 LE	1.8387	0.5166	29.48	0.5649	0.08	19.7

[a] a, e, i and H (semi-major axis, eccentricity, and inclination, respectively) were obtained using JPL Horizons.
[b] Diameter and albedo measurements were obtained from this work.

Table 1
Observational parameters.

Object	Date	UT	R.A.[a]	Dec.[a]	r (AU)[a]	Δ (AU)[a]	φ (°)[a]	V-mag[a]
2007 LE	06/03/12	11:08–12:17	15 35 49.40	+00 57 47.2	1.058	0.0495	27.72	14.53

[a] Observational properties were obtained from JPL Horizons.

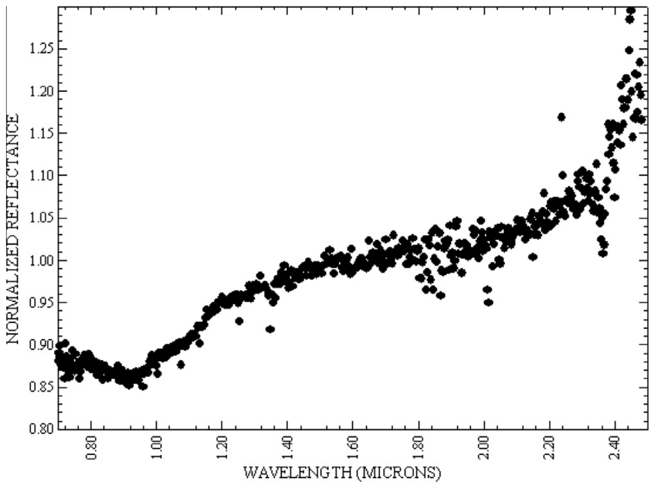

Fig. 1. The solar corrected near-infrared spectra of 2007 LE was normalized to unity at 1.5 µm. Visible data was not available to augment the near-infrared.

and Singer (1986). Using the calculations of Sanchez et al. (2012) for ordinary chondrites, the Band I center change would be 0.0003 µm. Since this small shift is significantly smaller than the uncertainty in the band center, no temperature corrections were made to the measured band center position.

Gaffey et al. (2002) developed formulas for determining pyroxene chemistries [iron (Fs) and calcium (Wo) contents] from the measured centers of the absorption bands near 1 µm (Band I) and 2 µm (Band II) in reflectance spectra of terrestrial, meteoritic, and lunar pyroxene and olivine plus pyroxene assemblages. Separate calibrations were derived for single pyroxene (e.g., basaltic achondrites) and two pyroxene (e.g., ordinary chondrite assemblages). The derived pyroxene compositions represent the average pyroxene mineralogies of the object being analyzed. The "single pyroxene" calibration formula of Gaffey et al. (2002) were tested by Burbine et al. (2007, 2009) using band parameters derived from several HED spectra. The "two pyroxene" calibration was tested using the Dunn et al. (2010) band parameters for ordinary chondrites. The Gaffey et al. (2002), Burbine et al. (2007, 2009), and Dunn et al. (2010) formulas regularly predict, within the error bars of each other, the iron (Fs) and calcium (Wo) content of the meteorite assemblages used in each study.

There is no discernable Band II in the 2007 LE spectrum. The increase in apparent reflectance beyond ~2.2 µm is not the long wavelength edge of a Band II feature but is rather the short wavelength edge of the thermal emission curve from the relatively warm asteroid surface. This thermal emission can be used to derive the surface albedo of the asteroid based on a technique pioneered by Abell et al. (2002), Abell (2003) and Rivkin et al. (2005). The technique models the thermal emission at a selected wavelength (in this case at 2.4 µm which is within the range of the SpeX instrument in the low resolution mode) for a spherical body with a range of albedos that is located at the heliocentric distance and phase angle at which the NEO was observed. The result is the thermal excess as a function of albedo. For a spectrum with no discernable Band II, the reflectance curve is assumed to be linear beyond ~1.5 µm. The excess above this linear trend at 2.4 µm is assumed to be thermal emission, and its value is compared to the function derived from the thermal models to derive the albedo. Based on its VNIR spectrum, the derived albedo of 2007 LE is ~8%.

If the absolute magnitude (H) and geometric visual albedo (Pv) are known then an effective diameter (km) can be calculated. Using equations developed by Fowler and Chillemi (1992) and Pravec and Harris (2007) the effective diameter (D_{eff}) can be calculated by the following equation:

$$D_{\mathrm{eff}} = [1329/(\mathrm{Pv})^{1/2}] * 10^{-(H/5)}$$

The JPL Small-Body Database Browser gives an H value of 19.7 (http://ssd.jpl.nasa.gov/sbdb.cgi?sstr=2007%20LE) which for an albedo of 0.08 corresponds to an effective diameter of 0.54 km. Radar observations by Goldstone and Arecibo derived an estimated diameter of 500 m (IAUC CBET Telegram 3175). Using this diameter and H = 19.7, a visual albedo of 0.093 is derived. Given the preliminary nature of the currently available radar derived diameters, this is in good agreement with the albedo derived from the VNIR spectrum. The VNIR albedo and diameter determinations are consistent with albedo and diameter measurements reported by the NASA Small Bodies Node of the Planetary Data System (Johnston, 2013).

Once the mineralogy and albedo of the asteroid are determined, a comparison can be made with the mineralogy, spectra, and cosmic ray exposure ages of meteorites in the terrestrial collections. Cosmic ray exposure (CRE) ages represent the time the parent meteoroid spent in space as a meter-scale object after ejection from its parent asteroid. CRE ages are a function of the physical strength of the meteoroid (lifetime against collisional disruption) and of the dynamical pathway (time scale to an Earth-crossing orbit). So, if the asteroid mineralogy can be linked to a specific meteorite type which bears an appropriate cosmic ray exposure age for delivery from that asteroid, a case can be made that the proposed asteroid is the probable parent body for that meteorite type because it matches the two key criteria for being a probable parent body: (1) mineralogy and (2) delivery mechanism which provides the appropriate flux and age distribution.

3. Analysis and interpretation

2007 LE exhibits a 1-µm absorption feature which can be associated with mafic silicate assemblages. The band center was measured relative to a linear continuum fitted tangent to the spectral curve outside the absorption feature (e.g., Cloutis et al.,

Table 3
Mineralogical parameters.

Asteroid	Band I (µm)	Albedo (%)	Fs	Fa	Meteorite affinity
2007 LE	0.94 ± .02	.08[a]	17 ± 1.4[d]	19 ± 1.3[d]	*Rose City*
(6) Hebe	0.933 ± .02	0.268[b] ± 0.008	16.8[e]		H-chondrites/IIE irons
(6) Hebe	0.933 ± .02	0.268[b] ± 0.008	17 ± 1.4[d]	15 ± 1.3[d]	H-chondrites/IIE irons
Rose City	NA	.065[c]	16.3 ± 1.2[f]	18.5 ± 0.5[f]	Black H-chondrite

[a] Albedo of 2007 LE from current work.
[b] Albedo of (6) Hebe from IRAS Minor Planet Survey V.6.
[c] The albedo of *Rose City* was the reflectance at 0.56 µm obtained from Gaffey (1976).
[d] Fs and Fa value were computed using the calibration of Dunn et al. (2010).
[e] Fs computed using calibration of Gaffey et al. (2002).
[f] Fs and Fa were obtained from SEM measurements on *Rose City* by Fruland (1975).

1986). The use of a straight-line continuum follows the procedure used to derive the most commonly used interpretive calibrations from laboratory spectra of meteorites (e.g., Adams, 1974, 1975; Cloutis et al., 1986; Cloutis and Gaffey, 1991; Gaffey et al., 1993, 2002; Gaffey and Gilbert, 1998; Dunn et al., 2010). The actual band center was determined by fitting several n-order polynomials to the feature. Based on the measured Band I center (0.94 μm), one can constrain a composition for the mafic surface components. Using the Dunn et al. (2010) equations, the pyroxene and olivine compositions would be $Fs_{17\pm1.4}$ and $Fa_{19\pm1.3}$, respectively. The absence of a detectable Band II precludes the use of the Gaffey et al. (2002) method for calculating pyroxene composition.

Based on the derived mineralogy of 2007 LE, the spectra of meteorite analogs that share similar/close to mineralogies were explored. Due to the lack of strong absorption features in both the 1- and 2-μm regions, the Howardite–Eucrite–Diogenite meteorite group was automatically eliminated as an option. The Pallasite meteorite group was not a viable option since the derived band center was not within wavelength range of the olivine dominated silicate assemblages present in pallasites. Additionally, the calculated albedo was too low for a pallasite-type assemblage. The Alcapolcoite–Lodranite meteorite group exhibits two relatively strong absorption features in the near-infrared not seen in the spectrum of 2007 LE. Additionally the pyroxene compositions of Acapulcoites and Lodranites ($Fs_{3.3-11.6}$ – e.g., Mittlefehldt et al., 1998; Patzer et al., 2004) is significantly lower than the pyroxene composition derived for 2007 LE. The Winonoaite meteorite group Fa and Fs values (Fa_{1-9}; Fs_{1-9}) are entirely out of range and the pyroxene component is primarily a calcium pyroxene with the near-infrared spectrum exhibiting two moderately deep absorption features. The Mesosiderite group is nearly a 50–50 mixture of pyroxene and Fe–Ni metal, rarely containing olivine. Mesosiderite spectra are difficult to obtain in the lab, however the known spectra show two very weak absorption bands. Mineralogy and spectral properties of the mesosiderites are inconsistent with the 2007 LE assemblage. The mineralogy of 2007 LE does not correlate well with the L- or LL-chondrite meteorite classes and their spectra are completely dissimilar. The band depth of the Band I feature of 2007 LE is much weaker than the Band I feature in ordinary chondrite spectra which also show a well-defined Band II feature. The silicate mineralogy of 2007 LE is consistent with an H-type ordinary chondrite but not with an L- or LL-type ordinary chondrite. However the absence of relatively strong Band I and Band II features in the 2007 LE spectrum eliminates a normal H-chondrite assemblage. Fig. 2A and B are comparison plots of 2007 LE and the aforementioned meteorite classes.

Among the ordinary chondrites, a subset of highly shocked specimens have low albedos and severely weakened absorption features (e.g., Heymann, 1967; Gaffey, 1976; Britt and Pieters, 1991, 1994; Keil et al., 1992). Asteroid 2007 LE's spectrum most resembles that of the black ordinary chondrites (e.g., *Farmington*, *Paragould*, *Rose City* – Fig. 2C), and in particular the *Rose City* meteorite. Fig. 3 plots 2007 LE and the black chondrite *Rose City* (Gaffey, 1976). The Band I absorption feature is consistent in position and depth with Rose City (7–9% deep), however it appears 2007 LE is a bit more olivine rich than Rose City. Mason and Wiik (1966) used the refractive indices of olivine and pyroxene in *Rose City* to determine their compositions as Fa_{19} and Fs_{15}, respectively. The Fa and Fs values were also calculated from compositions measured by an electron microprobe (Fruland, 1975). Those measurements indicated that the mean olivine and orthopyroxene compositions in *Rose City* were $Fa_{18.5\pm0.5}$ and $Fs_{16.3\pm1.2}$ (±1 sigma). The comparable compositions of H-chondrites are $Fs_{14.5-18}$ and Fa_{16-20}, for L-chondrites, Fs_{19-22} and Fa_{22-26}, and for LL-chondrites, Fs_{22-26} and Fa_{27-32}. A visual representation of this is shown in Fig. 4A and B (Figs. 3a and 4a of Dunn et al., 2010). The measured olivine

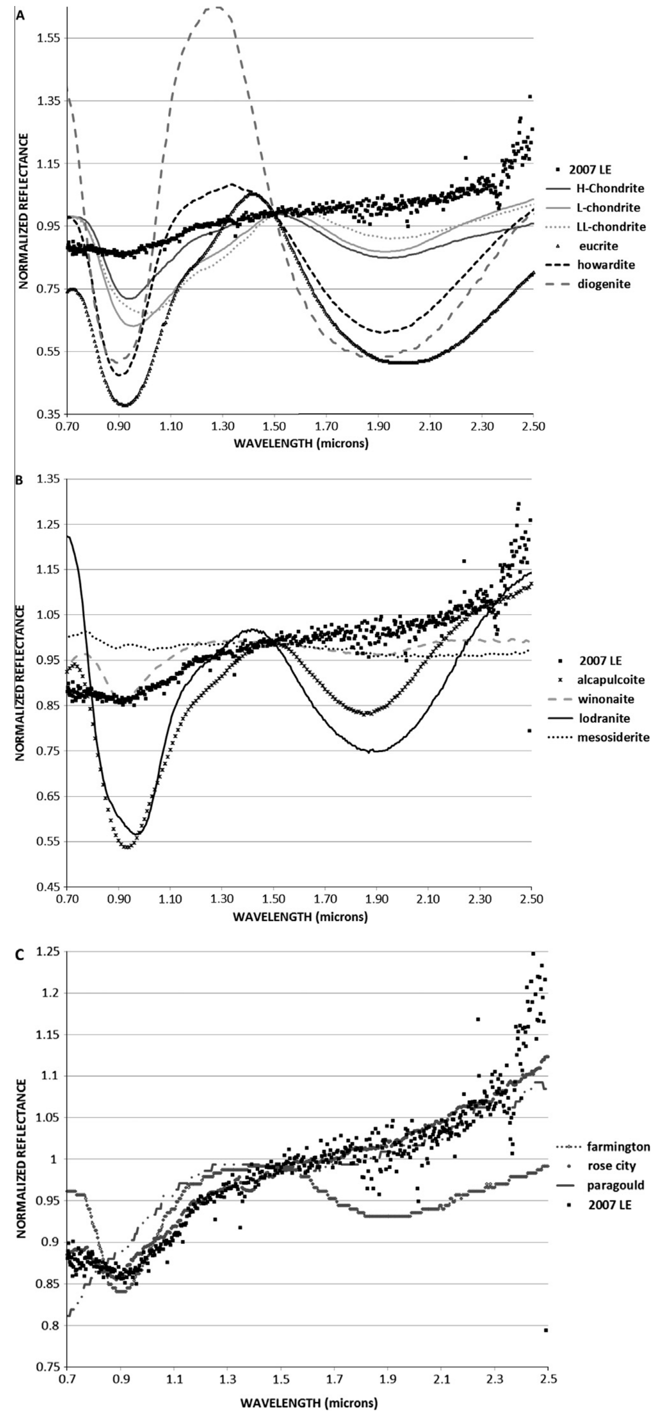

Fig. 2. Comparison plot of 2007 LE and the meteorite classes. The alcapulcoite, winonaite, lodranite meteorite spectra were retrieved from the Relab spectral database, 2007 LE is from this work, and the remaining spectra were obtained from Gaffey (1976). All spectra were normalized to 2007 LE at 1.5 μm.

and pyroxene compositions of *Rose City* fall in the range of the H-chondrites. Both (*6*) Hebe and 2007 LE plot amongst the H-chondrites.

Fig. 5 plots our results on a graph of Fa versus Fs for the H, L and LL chondrite groups (after Fig. 4.2 in Dodd (1981)). We extracted the spectral band parameters for 2007 LE and (*6*) Hebe and used the Dunn et al. (2010) equations to calculate the Fa and Fs chemistries. Using these spectral parameters, essentially identical Fs values were derived from the Gaffey et al. (2002) calibration, however that calibration does not derive Fa values. For *Rose City*,

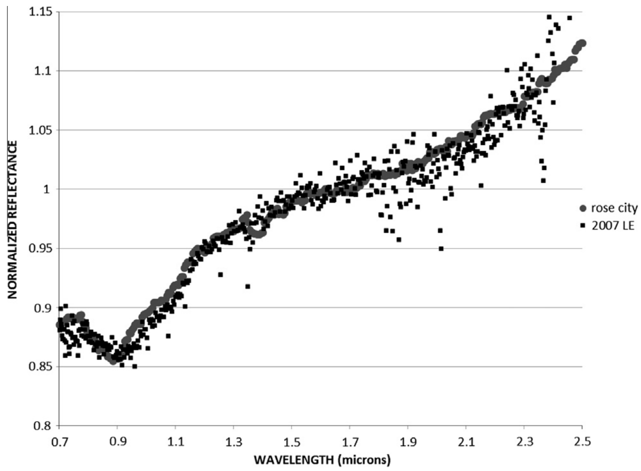

Fig. 3. The spectrum of 2007 LE and Gaffey's (1976) spectrum of the black chondrite *Rose City*. *Rose City* was normalized to 2007 LE over the 1.5–1.7 μm spectral interval. The Band I absorption feature is consistent in position and depth with *Rose City*, however it appears 2007 LE is a bit more olivine rich than *Rose City*. The intriguing thing about black chondrites is that they contain a fair percentage of olivine, but the shock has essentially squashed out any spectroscopic evidence of it – disordering the olivine in such a way that made it spectroscopically opaque. The increased upward curvature of the 2007 LE spectrum relative to the *Rose City* spectrum at the longest wavelengths (the 2007 LE spectrum crosses from below the *Rose City* spectrum shortwards of ∼2.3 μm to above the *Rose City* spectrum longwards of ∼2.3 μm) consistent with a thermal emission component in the 2007 LE spectrum.

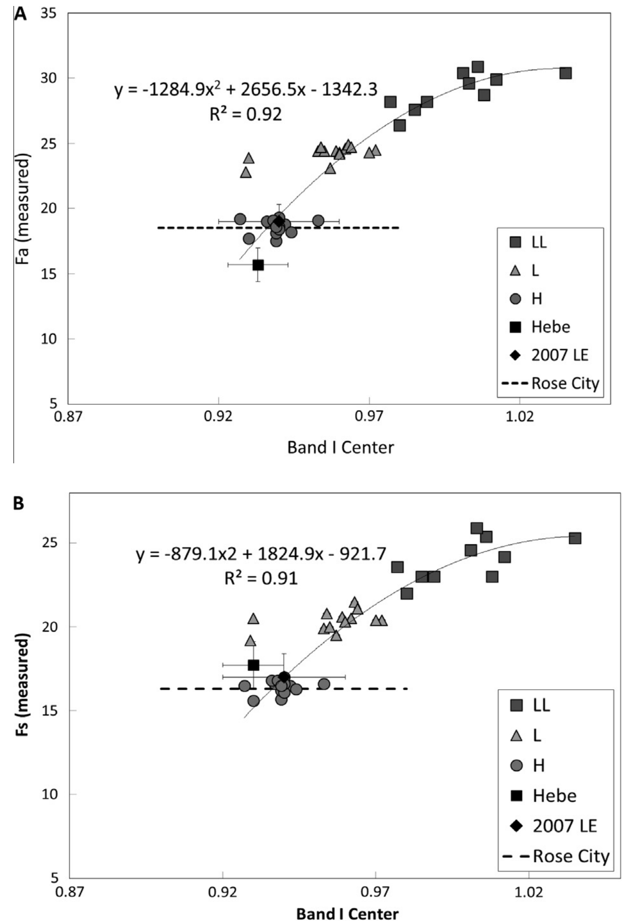

Fig. 4. Plot of Fa versus Band I center and Fs versus Band I center using derived band centers and Fa and Fs values of (6) Hebe, *Rose City*, and 2007 LE (Figs. 3a and 4a of Dunn et al., 2010). *Rose City* plots Fs and Fa values only, whilst (6) Hebe and 2007 LE plot amongst the H-chondrites.

we used the average Fa and Fs values derived from scanning electron microprobe measurements of individual grains made by Fruland (1975). Table 3 lists the extracted/derived values. (*6*) Hebe, *Rose City* and 2007 LE all plot within the H-chondrite group. Since the H-chondrites derive from a single main belt parent body (further discussion of this issue is provided in Section 4 of the paper), the slight offsets of Hebe, 2007 LE and *Rose City* from each other, could represent slightly different lithologies on/from the H-chondrite parent body.

Rose City is a very complex H-chondrite with H5 and H6 lithologies, which experienced shock, brecciation, and recrystallization (Fruland, 1975). The H-chondrite parent material was shocked to between 45 and 90 GPa (Stöffler et al., 1991) at ∼380 and ∼2300 Myr ago (Bogard, 1995). The shock effects noted in the meteorite are heterogeneous and reflect the uneven distribution of high temperatures and pressures during the shock event (Fruland, 1975). Shocking the ordinary chondrite assemblage produces structural disordering of the olivine crystal structure that essentially make it increasingly optically opaque, which will affect the Band I position by decreasing the effective spectral abundance of olivine shifting the band center towards shorter wavelengths (Britt et al., 1989) So, it is inferred the more shock a body has experienced, the more disordered are the crystals masking the true mineralogy.

We suggest *Rose City* has experienced shock to a higher degree than that of, 2007 LE. The various portions of the much larger (∼0.5 km) 2007 LE body is very likely to have experienced a wider range of shock intensities than the ∼10 kg *Rose City* sample. The less shocked components of 2007 LE would have higher albedos and contribute disproportionally to the spectral reflectance. 0.5 km bodies undergo what are called "YORP-cycles", where their spin axes orientations can flip from prograde to retrograde or vice versa. This means the timescales to get out of the main belt can be very long in some cases and such timescales, ∼380 My are not unreasonable for this object, however proving that the shock event on (*6*) Hebe is related to the ejection event is difficult if not impossible at this given time.

The black chondrites are ordinary chondrites that have experienced strong shock events that dramatically lowered their albedo. The mineralogy comprising black chondrites is essentially that of the ordinary chondrites as far as the metal content and olivine/pyroxene compositions (Gaffey, 1976). Spectrally, they are influenced by the opaque minerals (troilite and Fe–Ni metal blebs) dispersed throughout the matrix and by shock blackened olivine (Britt and Pieters, 1991, 1994). Black chondrites are characterized by high shock, low gas retention, overall low reflectance values, subdued absorption features, and a flattened spectrum (Britt and Pieters, 1991, 1994).

2007 LE's albedo of 0.08 (this work) and *Rose City*'s albedo of 0.065 (reflectance at 0.56 μm – Gaffey, 1976) are consistent within their uncertainties and further support the compositional link. The effective diameter of 2007 LE (∼0.5 km) indicates it was a fragment of a larger object which underwent a shock event. 2007 LE is a portion of a region of highly shocked material on that chondritic parent body. Compared to other shock blackened chondrites, the relatively slow cooling rate of *Rose City* (Yolcubal et al., 1997) is consistent with a greater depth and a larger volume of shocked material on the parent body. Ejecting a ∼0.5 km fragment whose surface and possibly interior is dominated by highly shocked material from that large shocked volume is thus plausible. Conversely, the size of 2007 LE is small enough that it need not sample a spectroscopically abundant lithology on its parent body (e.g. Keil et al., 1992).

Theoretical models indicate that the majority of asteroidal material delivered to the inner Solar System (and to the Earth)

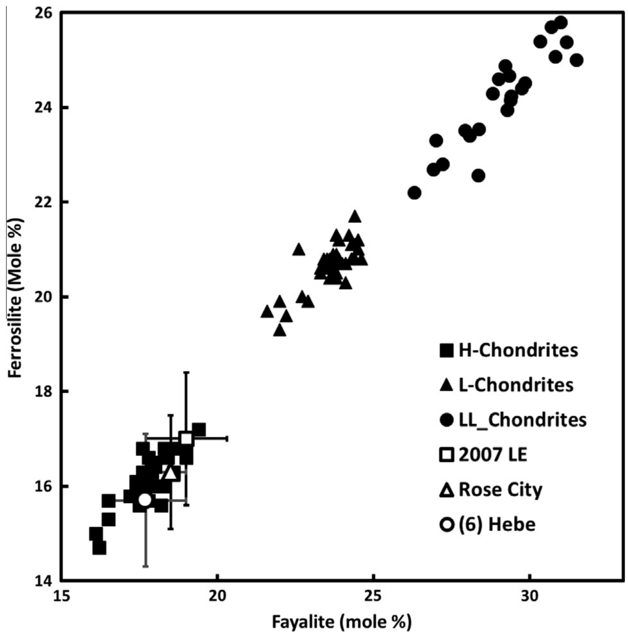

Fig. 5. Fa and Fs value results plotted with the H-, L-, and LL-type ordinary chondrites from Keil and Fredriksson (1964) and Hayse (1978). 2007 LE, *Rose City* and (*6*) Hebe plot within the H-chondrite cluster. The "error bars" on the (*6*) Hebe and 2007 LE points represent estimated uncertainties in the determinations in mineral compositions. The "error bars" on the *Rose City* point represent the one standard deviation spread in the measured mineral compositions in the specimen.

originates from the 3:1 mean motion resonance and the υ_6 secular resonance (e.g., Wisdom, 1985; Froeschle and Scholl, 1986, 1993; Yoshikawa, 1990; Farinella et al., 1993a, 1993b, 1994; Froeschle and Morbidellil, 1993; Hadjidemetriou, 1993; Moons and Morbidelli, 1995; Morbidelli and Moons, 1995; Rabinowitz, 1997; Michel et al., 1996a, 1996b; Gladman et al., 1997; Migliorini et al., 1997; Morbidelli and Gladman, 1998; Michel and Froeschle, 2000; Bottke et al., 2002; Ji and Liu, 2007; Welten et al., 2010). Specific dynamical simulations of test bodies ranging in size from several meters to kilometers with orbital elements similar to near resonance asteroids as well family clusters have been conducted and were deemed capable of being inserted into the mean motion and secular resonances through a variety of pathways including direct injection or slowly drifting into a resonance via Yarkovsky thermal forces (whose strength and direction are influenced by the Yarkovsky–OKeefe–Radzievskii–Paddack (YORP) effect), (Yoshikawa, 1987; Scholl and Froeschle, 1990, 1991; Farinella et al., 1993a; Morbidelli et al., 1994; Vokrouhlicky and Farinella, 1998, 1999; Bottke et al., 2001, 2005, 2006, 2009; Nesvorný et al., 2007; Carruba and Michtchenko, 2009; Carruba, 2010; Tsiganis, 2010; Carruba and Morbidelli, 2011). The delivery timescale to these resonance varies with the starting location and size of the precursor; some could reach a resonance within a few Myr, while others could take tens to hundreds of Myr. Once in the resonance, the orbits either evolve to collisions with the Sun, hyperbolic ejection from the Solar System, or planet crossing orbits (e.g.: Ito and Malhotra, 2004; Michel et al., 2005; Tsiganis, 2010; Carruba et al., 2011). The time scale for these bodies to reach an endstate is between a few Myr and a few tens of Myr.

The orbital evolution of the majority of meteoroids liberated from their parent asteroid are governed by the Yarkovsky effects and YORP, which are key in delivering bodies ($D < 20$ km) from their source region to the chaotic zones capable of moving material into near-Earth space (Bottke et al., 2001). These fragments spend a majority of their dynamical lifetime undergoing a weak semimajor axis evolution in the main belt region, which accounts for the paucity of short cosmic ray exposure ages seen among the stony meteorites (Bottke et al., 2006). Dynamical studies have shown the primary sources of Mars-crossing bodies and near-Earth objects are the υ_6 secular and 3:1 mean-motion resonances, along with a plethora of tiny resonances stacked up in the innermost region of the main belt (Bottke et al., 2006). In the border region of the υ_6, orbital evolution is subject to Mars encounters before entering NEO space and the time required increases with distance from the resonance (Michel et al., 2005). Of particular interest are the bodies that are transferred into Earth-crossing orbits. The shallow size distribution of NEOs suggests collisional injection into the resonance is not the key mechanism supplying the population (i.e., crater ejecta tends to have a very steep size distribution, which is not observed). Instead, an interplay between collisions, Yarkovsky, and YORP act together to bring a robust number of fragments into the resonances (Bottke et al., 2006). Once in near-Earth space the lifetime of an NEO is on the order of ~6.5 Myr with numerical simulations suggesting 37% of kilometer-sized NEOs derive from the υ_6 secular resonance (Bottke et al., 2002). Estimates suggest that 55 ± 18 objects with $H < 18$ ($D > \sim 1$ km for S-type albedos) make their way into the υ_6 secular resonance every million years (Bottke et al., 2002).

4. Discussion

2007 LE was identified as a binary asteroid system by Brozovic et al. (2012). The secondary could have been the result of the event which ultimately caused 2007 LE to release the *Rose City* meteoroid. Isotopic and mineralogical studies of the H-chondrites suggest that they all derive from a single parent body (Trieloff et al., 2003; Wittmann et al., 2010; Henke et al., 2012). However, recent spectroscopic evidence has put this assertion into question. As part of the 3:1 Kirkwood Gap survey, Fieber-Beyer et al. (2011) identified (*695*) Bella as an H-chondrite body, and in Fieber-Beyer and Gaffey (2014), three additional H-chondrite bodies were mineralogically identified [(*1064*) Aethusa, (*1166*) Sakuntula, and (*1607*) Mavis]. This small subset of H-chondrite like asteroids were suggested as a possible old, dispersed asteroid family belonging to (*6*) Hebe (Gaffey and Fieber-Beyer, 2013). Complementing the existing and ever growing list of H-chondrite candidates near the 3:1 Kirkwood Gap, Vernazza et al. (2014) identified several additional asteroids as viable H-chondrite candidates. Furthermore, Burbine et al. (2002) make the point that there may be several H chondrite asteroids from the original parent body. This leaves several options: (1) (*6*) Hebe may have an old dispersed family that is the source of the meteorite, (2) another parent asteroid or asteroid family with H chondrite-like properties is the true source of the H chondrites, (3) the H chondrites come from multiple parent bodies, with all of these asteroids condensed from the same nebular compositional reservoir; a conclusion at odds with the meteorite data which point to a single H-chondrite parent body (McCoy, 2010, personal communication; Trieloff et al., 2003; Wittmann et al., 2010; Henke et al., 2012).

The *Rose City* meteorite has been identified as an H5 S6 shock blackened ordinary chondrite (Mason and Wiik, 1966; Yolcubal et al., 1997), however it contains shocked clasts of H6 lithology as well (Fruland, 1975). H-chondrite breccias commonly contain petrographic types 4–6 indicating impacts onto an originally "onion-shell" H-chondrite parent body sufficient to excavate relatively deep-seated materials. *Rose City* could be a fragment of the H-chondrite parent body identified as (*6*) Hebe (Gaffey and Gilbert, 1998; Bottke et al., 2010).

Computational models, based on dynamical physics, indicate the majority of asteroidal material are delivered to Earth from the 3:1 mean motion resonance (Morbidelli and Gladman, 1998).

This makes the 3:1 resonance a likely candidate source region for the H-chondrites, which constitute approximately a third of all meteorite falls. Accordingly, because Hebe fragments can readily reach the 3:1 resonance, we must consider Hebe a reasonable candidate to be the source of the H chondrites. Proving Hebe fragments dominate all other H chondrite-like sources, however, is a difficult task.

The CRE age of the *Rose City* meteorite calculated by Graf and Marti (1995) of ~39 Myr is the interval where it was free-floating in space as a body smaller than a few meters in size. This long timescale means that making a direct connection between an NEO and a meteorite fall is challenging. The orbit of the NEO 2007 LE, with $a = 1.84$ AU, $e = 0.5$, and $i = 29°$, gives us the impression that it has been interacting with the quasi-stable Hungaria region for some time. This would allow it to have a long lifetime in the inner Solar System. One can postulate a connection between *Rose City* and 2007 LE on this basis, with the former released from the latter while 2007 LE was residing on such orbits. If *Rose City* were to have been sitting on the surface on 2007 LE until recent times, it would probably show 39 My of 2π exposure, however it is believed that the CRE age in this case represents 4π exposure. Furthermore, if *Rose City* was liberated from 2007 LE 39 My ago, this would allow 39 My for the bodies to evolve to very different orbits. This is an enormous interval in the inner Solar System considering NEO orbits can dynamically diverge from one another on timescales of a few hundred years (i.e., this is why we cannot predict future NEO orbits or Earth impacts more than a few hundred years out from today). Our conclusion is that we cannot prove a dynamical link between the two bodies given the available data. The best interpretation is that 2007 LE and *Rose City* have a compositional link, and both could come from the same parent body/family, which could plausibly be (6) Hebe.

Acknowledgments

The authors would like to thank David O'Brien and the anonymous reviewers whose insight and suggestions greatly improved the paper. Portions of this work were supported by the NASA Near-Earth Objects Observations/Planetary Astronomy Program grant NNX12AG12G and by the NASA Planetary Geology and Geophysics Program Grant NNX11AN84G.

References

Abell, P.A., 2003. Near-IR Reflectance Spectroscopy of Near-Earth Objects: A Study of Their Compositions, Meteorite Affinities, and Source Regions. Ph.D. Diss., Rensselaer Polytechnic Institute.

Abell, P.A., Gaffey, M.J., Hardersen, P.S., 2002. Spectral rotational variation and meteorite affinities of the potentially hazardous Asteroid 1998 ST27. Asteroids, Comets, Meteors. Abstract 18-070.

Adams, J.B., 1974. Visible and near-infrared diffuse reflectance spectra of pyroxenes as applied to remote sensing of solid objects in the Solar System. J. Geophys. Res. 79, 4829–4836.

Adams, J.B., 1975. Interpretation of visible and near-infrared diffuse reflectance spectra of pyroxenes and other rock-forming minerals. In: Karr, C. (Ed.), Infrared and Raman Spectroscopy of Lunar and Terrestrial Minerals. Academic Press, New York, pp. 91–116.

Binzel, R.P., Rivkin, A.S., Stuart, J.S., Harris, A.W., Bus, S.J., Burbine, T.H., 2004. Observed spectral properties of near-Earth objects: Results for population distribution, source regions, and space weathering processes. Icarus 170, 259–294.

Bogard, D.D., 1995. Impact ages of meteorites: A synthesis. Meteoritics 30, 244–268.

Bottke Jr., W.F., Vokrouhlický, D., Brož, M., Nesvorný, D., Marbidelli, A., 2001. Dynamical spreading of asteroid families by the Yarkovsky effect. Science 294, 1693–1696.

Bottke, W.F., Morbidelli, A., Jedicke, R., Petit, J.M., Levison, H.F., Michel, P., Metcalfe, T.S., 2002. Debiased orbital and size distribution of the near-Earth objects. Icarus 156, 399–433.

Bottke, W.F., Durda, D.D., Nesvorny, D., Jedicke, R., Morbidelli, A., Vokrouhlicky, D., Levison, H.F., 2005. Linking the collisional history of the main asteroid belt to its dynamical excitation and depletion. Icarus 179, 63–94.

Bottke Jr., W.F., Vokrouhlický, D., Rubincam, D.P., Nesvorný, D., 2006. The Yarkovsky and Yorp effects: Implications for asteroid dynamics. Annu. Rev. Earth Planet. Sci. 34, 157–191.

Bottke, W.F., Nesvorný, D., Vokrouhlický, D., Morbidelli, A., 2009. The Gefion family as the probable source of the L chondrite meteorites. Lunar Planet. Sci. XL. Abstract #1445.

Bottke, W.F., Vokrouhlický, D., Nesvorný, D., Shrbeny, L., 2010. (6) Hebe really is the H chondrite parent body. In: 42nd DPS Meeting, Pasadena, CA. Abstract 46.06.

Britt, D.T., Pieters, C.M., 1991. Black ordinary chondrites: An analysis of abundance and fall frequency. Meteoritics 26, 279–285.

Britt, D.T., Pieters, C.M., 1994. Darkening in black and gas-rich ordinary chondrites: The spectral effects of opaque morphology and distribution. Geochim. Cosmochim. Acta 58, 3905–3919.

Britt, D.T., Pieters, C.M., Petaev, M.I., Zaslavskaya, N.I., 1989. The Tsarev meteorite: Petrology and bidirectional reflectance spectra of a shock-blackened L chondrite. Proc. Lunar Sci. Conf. 19, 537–545.

Brozovic, M. et al., 2012. Announced June 2012 CBET 3175.

Burbine, T.H., McCoy, T.J., Meibom, A., Gladman, B., Keil, K., 2002. Meteoritic parent bodies: Their number and identification. In: Bottke, W.F., Jr., Cellino, A., Paolicchi, P., Binzel, R.P. (Eds.), Asteroids III. University of Arizona Press, Tucson, pp. 653–667.

Burbine, T.H., McCoy, T.J., Jarosewich, E., Sunshine, J.M., 2003. Deriving asteroid mineralogies from reflectance spectra: Implications for the MUSES-C target asteroid. Antarct. Meteorite Res. 16, 185–195.

Burbine, T.H, Buchanan, P.C., Binzel, R.P., 2007. Deriving formulas from HED spectra for determining the pyroxene mineralogy of Vesta and Vestoids. Lunar Planet. Sci. XXXVIII. Abstract 2117.

Burbine, T.H., Buchanan, P.C., Dolkar, T., Binzel, R.P., 2009. Pyroxene mineralogies of near-Earth Vestoids. Meteorit. Planet. Sci. 44, 1331–1341.

Carruba, V., 2010. Dynamical erosion of asteroid groups in the region of the Phocaea family. Mon. Not. R. Astron. Soc. 403, 1834–1848.

Carruba, V., Michtchenko, T.A., 2009. A frequency approach to identifying asteroid families II: Families interacting with nonlinear secular resonances and low order mean-motion resonances. Astron. Astrophys. 493, 267–292.

Carruba, V., Morbidelli, A., 2011. On the first υ_6 anti-aligned liberating asteroid family of Tina. Mon. Not. R. Astron. Soc. 412, 2040–2051.

Carruba, V., Machuca, J.F., Gasparino, H.P., 2011. Dynamical erosion of asteroid groups in the region of the Pallas family. Mon. Not. R. Astron. Soc. 412, 2052–2062.

Clark, R.N., 1980. A large-scale interactive one-dimensional array processing system. Publ. Astron. Soc. Pacific 92, 221–224.

Cloutis, E.A., Gaffey, M.J., 1991. Pyroxene spectroscopy revisited: Spectral-compositional correlations and relationship to geothermometry. J. Geophys. Res.: Planets 96, 22809–22826.

Cloutis, E.A., Gaffey, M.J., Jackowski, T.L., Reed, K.L., 1986. Calibration of phase abundance, composition, and particle size distribution for olivine–orthopyroxene mixtures from reflectance spectra. J. Geophys. Res. 91, 11641–11653.

DeMeo, F.E., Binzel, R.P., Slivan, S.M., Bus, S.J., 2009. An extension of the Bus asteroid taxonomy into the near-infrared. Icarus 202, 160–180.

Dodd, R.T., 1981. Meteorites: A Petrologic-Chemical Synthesis. Cambridge Univ. Press, New York.

Dunn, T.L., McCoy, T.J., Sunshine, J.M., McSween Jr., H.Y., 2010. A coordinated mineralogical, spectral, and compositional study of ordinary chondrites: Implications for asteroid spectroscopic classification. Icarus 208, 789–797.

Farinella, P., Gunczi, R., Froeschlé, Ch., Froeschlé, C., 1993a. The injection of asteroid fragments into resonances. Icarus 101, 174–187.

Farinella, P., Froeschle, C., Gonczi, R., 1993b. Meteorites from the Asteroid 6 Hebe. Celest. Mech. Dynam. Astron. 56, 287–305.

Farinella, P., Froeschlé, Ch., Froeschlé, C., Gonczi, R., Hahn, G., Morbidelli, A., Valsecchi, B., 1994. Asteroids falling onto the Sun. Nature 371, 314–317.

Fevig, R.A., Fink, U., 2007. Spectral observations of 19 weathered and 23 fresh NEAs and their correlations with orbital parameters. Icarus 188, 175–188.

Fieber-Beyer, S.K., 2010. Mineralogical Characterization of Asteroids in/near the 3:1 Kirkwood Gap. Ph.D. Dissertation, University of North Dakota, Grand Forks. 203pp.

Fieber-Beyer, S.K., Gaffey, M.J., 2014. Near-infrared spectroscopy of 3:1 Kirkwood Gap asteroids II: Probable and plausible parent bodies; primitive and differentiated. Icarus 229, 99–108.

Fieber-Beyer, S.K., Gaffey, M.J., Kelley, M.S., Reddy, V., Reynolds, C.M., Hicks, T., 2011. The Maria asteroid family: Genetic relationships and a plausible source of mesosiderites near the 3:1 Kirkwood Gap. Icarus 213, 524–537.

Fowler, J.W., Chillemi, J.R., 1992. IRAS Asteroid Data Processing: The IRAS Minor Planet Survey, Philips Laboratory Technical Report PL-TR-92-2049. Jet Propulsion Laboratory, Pasadena, California, pp. 17–43.

Froeschle, Ch., Morbidellil, M., 1993. The secular resonances in the Solar System. Asteroids Comets Meteors, 189–204.

Froeschle, Ch., Scholl, H., 1986. The secular resonance υ_6 in the asteroid belt. Astron. Astrophys. 166, 326–332.

Froeschle, Ch., Scholl, H., 1993. Numerical experiments in the 3:1 and υ_6 overlapping resonance region. Celest. Mech. Dynam. Astron. 56, 163–176.

Fruland, R.M., 1975. Impact Generated Volatile Movement and Redistribution in the Rose City Meteorite. M.S. Thesis, University of North Dakota, Grand Forks. 120pp.

Gaffey, M.J., 1976. Spectral reflectance characteristics of the meteorite classes. J. Geophys. Res. 81, 905–920.

Gaffey, M.J., Fieber-Beyer, S.K., 2013. Identification of a possible H-chondrite asteroid family. Meteorit. Planet. Sci. Suppl., id.5124.
Gaffey, M.J., Gilbert, S.L., 1998. Asteroid 6 Hebe: The probable parent body of the H-type ordinary chondrites & the IIE iron meteorites. Meteorit. Planet. Sci. 33, 1281–1295.
Gaffey, M.J., Reed, K.L., Kelley, M.S., 1992. Relationship of E-type Apollo Asteroid 3103 (1982 BB) to the enstatite achondrite meteorites and the Hungaria asteroids. Icarus 100, 95–109.
Gaffey, M.J., Bell, J.F., Brown, R.H., Burbine, T.H., Piatek, J., Reed, R.L., Chaky, D.A., 1993. Mineralogic variations within the S-type asteroid class. Icarus 106, 573–602.
Gaffey, M.J., Cloutis, E.A., Kelley, M.S., Reed, K.L., 2002. Mineralogy of asteroids. In: Bottke, W.F., Cellino, A., Paolicchi, P., Binzel, R.P. (Eds.), Asteroids III. Univ. of Arizona Press, pp. 183–204.
Gastineau-Lyons, H.K., McSween Jr., H.Y., Gaffey, M.J., 2002. A critical evaluation of oxidation versus reduction during metamorphism of L and LL group chondrites, and implications for asteroid spectroscopy. Meteorit. Planet. Sci. 37, 75–89.
Gladman, B.J. et al., 1997. Dynamical lifetimes of objects injected into asteroid belt resonances. Science 277, 197–201.
Graf, T., Marti, K., 1995. Collisional history of H-chondrites. J. Geophys. Res. 100, 21247–21263.
Hadjidemetriou, J.D., 1993. Asteroid motion near the 3:1 resonance. Celest. Mech. Dynam. Astron. 56, 563–599.
Hardersen, P.S., Gaffey, M.J., Abell, P.A., 2005. Near-IR spectral evidence for the presence of iron-poor orthopyroxenes on the surfaces of six M-type asteroids. Icarus 175, 141–158.
Hayse, J.V., 1978. The metamorphic history of LL-group ordinary chondrites. Earth Planet. Sci. Lett. 40, 365–381.
Henke, S., Gail, H.-P., Trieloff, M., Schwarz, W.H., Kleine, T., 2012. Thermal history modelling of the H chondrite parent body. Astron. Astrophys. 545, A135.
Heymann, D., 1967. On the origin of hypersthene chondrites: Ages and shock effects of black chondrites. Icarus 6, 189–221.
Hinrichs, J.L., Lucey, P.G., 2002. Temperature-dependent near-infrared spectral properties of minerals, meteorites, and lunar soil. Icarus 155, 169–180.
Ito, T., Malhotra, R., 2004. Near-Earth orbital distribution of asteroid fragments coming from the υ_6 resonance. In: 35th COSPAR Scientific Assembly, Paris, France, p. 3622.
Ji, J., Liu, L., 2007. Revisit of dynamical mechanisms of transporting asteroids in the 3:1 resonance to near-Earth space. Chin. J. Astron. Astrophys. 7, 148–154.
Johnston, W.R., 2013. Binary Minor Planets V6.0. EAR-A-COMPIL-5-BINMP-V6.0. NASA Planetary Data System.
Keil, K., Fredriksson, K., 1964. The iron, magnesium, and calcium distribution in coexisting olivines and rhombic pyroxenes of chondrites. J. Geophys. Res. 69, 3487–3515.
Keil, K., Bell, J.F., Britt, D.T., 1992. Reflection spectra of shocked ordinary chondrites and their relationship to asteroids. Icarus 98, 43–53.
Lucey, P.G., Keil, K., Whitely, R., 1998. The influence of temperature on the spectra of the A-asteroids and implications for their silicate chemistry. J. Geophys. Res.: Planets 103, 5865–5871.
Mainzer, A. et al., 2012. Physical parameters of asteroids estimated from the wise 3-band data and NEOWISE post-cryogenic survey. Astrophys. J. 760, L12.
Mason, B., Wiik, H.B., 1966. The composition of the Bath, Frankfort, Kakangari, Rose City, and Tadjera meteorites. Am. Mus. Novit. 2272, 1–24.
McCord, T.B., Adams, J.B., Johnson, T.V., 1970. Asteroid Vesta: Spectral reflectivity and compositional implications. Science 168, 1445–1447.
Michel, P., Froeschle, C.H., 2000. Dynamics of small Earth-approachers on low eccentricity orbits and implications for their origins. Celest. Mech. Dynam. Astron. 78, 93–112.
Michel, P., Farinella, P., Froeschle, Ch., 1996a. Dynamical evolution of NEAs: Close encounters, secular perturbations and resonances. Earth Moon Planets 72, 151–164.
Michel, P., Farinella, P., Froeschle, Ch., 1996b. The orbital evolution of the asteroid Eros and implications for collision with the Earth. Nature 380, 689–691.
Michel, P., Morbidell, A., Bottke, W.F., 2005. Origin and dynamics of near Earth objects. C.R. Phys. 6, 291–301.
Migliorini, F., Morbidelli, A., Zappala, V., Gladman, B.J., Bailey, M.E., Cellino, A., 1997. Vesta fragments from υ_6 and 3:1 resonances: Implications for V-type near-Earth asteroids and howardite, eucrite, and diogenite meteorites. Meteorit. Planet. Sci. 32, 903–916.
Mittlefehldt, D.W., McCoy, T.J., Goodrich, C.A., Kracher, A., 1998. Non-chondritic meteorites from asteroidal bodies. In: Papike, J.J. (Ed.), Planetary Materials, vol. 36. Min. Soc. Am., Reviews in Mineralogy, pp. 4-1–4-195.
Moons, M., Morbidelli, A., 1995. Secular resonances in mean motion commensurabilities: The 4/1, 3/1, 5/2, and 7/3 cases. Icarus 114, 33–50.
Morbidelli, A., Moons, M., 1995. Numerical evidence on the chaotic nature of the 3/1 mean motion commensurability. Icarus 115, 60–65.
Morbidelli, A., Gladman, B., 1998. Orbital and temporal distributions of meteorites originating in the asteroid belt. Meteorit. Planet. Sci. 33, 999–1016.
Morbidelli, A., Gonczi, R., Froeschle, Ch., Farinella, P., 1994. Delivery of meteorites through the ν6 secular resonance. Astron. Astrophys. 282, 955–979.
Moroz, L., Schade, U., Wäsch, R., 2000. Reflectance spectra of olivine–orthopyroxene bearing assemblages at decreased temperatures: Implications for remote sensing of asteroids. Icarus 147, 79–93.
Mueller, M. et al., 2011. ExploreNEOs. III. Physical characterization of 65 potential spacecraft target asteroids. Astron. J. 141, 109–117.
Nesvorný, D., Vokrouhlický, D., Bottke Jr., W.F., Gladman, B., Haggstrom, T., 2007. Express delivery of fossil meteorites from the inner asteroid belt to Sweden. Icarus 188, 400–413.
Nesvorný, D., Vokrouhlický, D., Morbidelli, A., Bottke, W.F., 2009. Asteroidal source of L chondrite meteorites. Icarus 200, 698–701.
Patzer, A., Hill, D.H., Boynton, W.V., 2004. Evolution and classification of acapulcoites and lodranites from a chemical point of view. Meteorit. Planet. Sci. 39, 61–85.
Pravec, R., Harris, A.W., 2007. Binary asteroid population. 1. Angular momentum content. Icarus 190, 250–259.
Rabinowitz, D.L., 1997. Are mainbelt asteroids a sufficient source for the Earth approaching asteroids? Predicted vs. observed orbital distributions. Icarus 127, 33–54.
Rayner, J.T. et al., 2003. SpeX: A medium-resolution 0.8–5.5 micron spectrograph and imager for the NASA Infrared Telescope Facility. Publ. Astron. Soc. Pacific 115, 362–382.
Reddy, V., 2009. Mineralogical Survey of near-Earth Asteroid Population: Implications for Impact Hazard Assessment and Sustainability of Life on Earth. Ph.D. Dissertation, University of North Dakota, Grand Forks. 355pp.
Reddy, V., Sanchez, J., Nathues, A., Moskovitz, N.A., Li, J.-Y., Cloutis, E.A., Archer, K., Tucker, R.A., Gaffey, M.J., Mann, J.P., Sierks, H., Schade, U., 2011. Photometric, spectral phase and temperature effects on Vesta and HED meteorites: Implications for DAWN mission. Icarus 217, 153–168.
Rivkin, A.S., Binzel, R.P., Bus, S.J., 2005. Constraining near-Earth object albedos using near-infrared spectroscopy. Icarus 175, 175–180.
Roush, T.L., 1984. Effects of Temperature on Remotely Sensed Mafic Mineral Absorption Features. MS Thesis, Univ. of Hawaii, Honolulu.
Roush, T.L., Singer, R.B., 1986. Gaussian analysis of temperature effects on the reflectance spectra of mafic minerals in the 1-μm region. J. Geophys. Res. 91, 10301–10308.
Rubin, A.E., Bottke, W.F., 2009. On the origin of shocked and unshocked CM clasts in H-chondrite regolith breccias. Meteorit. Planet. Sci. 44, 701–724.
Sanchez, J.A., Reddy, V., Nathues, A., Cloutis, E.A., Mann, P., Hiesinger, H., 2012. Phase reddening on near-Earth asteroids: Implications for mineralogical analysis, space weathering and taxonomic classification. Icarus 220, 36–50.
Scholl, H., Froeschle, Ch., 1990. Meteorites from the υ6 secular resonance. Asteroids Comets Meteors, 565–566.
Scholl, H., Froeschle, Ch., 1991. The υ_6 secular resonance region near 2 AU: A possible source of meteorites. Astron. Astrophys. 245, 316–321.
Stöffler, D., Keil, K., Scott, E.R.D., 1991. Shock metamorphism of ordinary chondrites. Geochim. Cosmochim. Acta 55, 3845–3867.
Sunshine, J.M., Bus, S.J., Corrigan, C.M., McCoy, T.J., Burbine, T.H., 2007. Olivine-dominated asteroids and meteorites: Distinguishing nebular and igneous histories. Meteorit. Planet. Sci. 42, 155–170.
Trieloff, M. et al., 2003. Structure and thermal history of the H-chondrite parent asteroid revealed by thermochronometry. Nature 422, 502–506.
Tsiganis, K., 2010. Dynamics of small bodies in the Solar System. Eur. Phys. J. Spec. Top. 186, 67–89.
Vernazza, P. et al., 2008. Compositional differences between meteorites and near-Earth asteroids. Nature 454, 858–860.
Vernazza, P. et al., 2014. Multiple and fast: The accretion of ordinary chondrite parent bodies. Astrophys. J. 791, 120 (22pp.).
Vokrouhlicky, D., Farinella, P., 1998. Orbital evolution of asteroidal fragments into the υ_6 resonance via Yarkovsky effects. Astron. Astrophys. 335, 351–362.
Vokrouhlicky, D., Farinella, P., 1999. The Yarkovsky seasonal effect on asteroidal fragments: A nonlinearized theory for spherical bodies. Astrophys. J. 118, 3049–3060.
Welten, K.C. et al., 2010. High porosity and cosmic ray exposure age of Asteroid 2008 TC3 derived from cosmogenic nuclides. Lunar Planet. Sci. 41. Abstract #2256.
Wisdom, J., 1985. A perturbative treatment of motion near the 3/1 commensurability. Icarus 63, 272–289.
Wittmann, A., Swindle, T.D., Cheek, L.C., Frank, E.A., Kring, D.A., 2010. Impact cratering on the H chondrite parent asteroid. J. Geophys. Res. 115, E07009. http://dx.doi.org/10.1029/2009JE003433.
Yolcubal, I., Sack, R.O., Wang, M.-S., Lipschutz, M.E., 1997. Formation conditions of igneous regions in ordinary chondrites: Chico, Rose City, and other heavily shocked H and L chondrites. J. Geophys. Res. 102 (E9), 21589–21611.
Yoshikawa, M., 1987. A simple analytical model for the secular resonance υ_6 in the asteroidal belt. Celest. Mech. 40, 233–272.
Yoshikawa, M., 1990. Motions of asteroids at the Kirkwood Gaps. Icarus 87, 78–102.